Electromagnetic Characterization of Broadband MEMS Antenna

Douglas A. Hutchings[1], Magda El-Shenawee[2] and Steve Tung[3]

[1] Microelectronics-Photonics Program
University of Arkansas, Fayetteville, AR 72701, USA
dwoten@uark.edu

[2] Department of Electrical Engineering
University of Arkansas, Fayetteville, AR 72701, USA
magda@uark.edu

[3] Department of Mechanical Engineering
University of Arkansas, Fayetteville, AR 72701, USA
chstung@uark.edu

Abstract: A broadband MEMS steerable antenna is fabricated on a silicon substrate using bulk micromachining techniques. The MEMS platform utilizes torsion hinges and is capable of rotation around two axes for full beam steering capabilities. The antenna was designed using the Ansoft High Frequency Structure Simulator (HFSS) package and operates between 10-16 GHz with a coplanar feedline routed across the MEMS platform hinges. The MEMS antenna performance was mechanically characterized and the results show the platform capable of rotations of 9.16° before failure. The scattering parameters were measured using a Vector Network Analyzer and shown to be in good agreement with the simulation results even when the platform is rotated.

Keywords: Broadband antenna, MEMS, mechanical steering, antenna measurements

1. Introduction

Reconfigurable MEMS antennas are antennas that can alter radiation, polarization and frequency characteristics by some change in the physical structure. Typically, reconfigurable antennas manipulate the operating frequency and radiation characteristics simultaneously. However, a system that can control the radiation characteristics without changing the operating frequencies has its advantages. The ability to change the radiation pattern while maintaining the operating frequencies could greatly enhance the system performance. Control of an antenna's radiation pattern can be used to avoid noise sources or intentional jamming, improve security by directing signals only toward intended users, serve as a switched diversity system, and expand

the beam steering capabilities of phased arrays. It is this problem that the proposed MEMS dual frame rotation platform seeks to address.

MEMS have been incorporated into antenna design and related components in a number of ways [1-4]. Four primary methods exist to utilize MEMS to reconfigure an antenna; the first method is to mechanically actuate the antenna and change its orientation [1]. The second method is to change the effective radiating structure [2]. The third method is to utilize MEMS capacitive switches to modify the impedance of the antenna [3], and the fourth method is to use MEMS phase shifters [4]. The current work is motivated by the mechanical actuation work reported in [1] as will be discussed in the following sections.

As known, the main beam of an antenna, or array of antennas, can be controlled in two ways; phase shifting elements or mechanical manipulation. Phase shifters are typically narrow band devices which limit the bandwidth of the final device. Mechanical steering on the other hand is not frequency limited but could be bulky. Therefore, combining mechanical rotation of individual antenna elements and traditional phase shifting techniques can lead to additional degrees of freedom for antenna array designers.

There is some work in the literature on integrating narrowband antennas with MEMS platforms [1]. To the best of the authors' knowledge, there is no work published for broadband antennas integrated onto a MEMS platform. The current work modified the methods in [1] to create a MEMS platform for a broadband planar antenna based on modification of the Fourpoint antenna reported in [5]. A coplanar waveguide (CPW) is routed across the silicon hinges of the platform to feed the antenna as will be discussed in Section 2. The antenna platform was created using bulk microfabrication techniques on a silicon substrate as proof-of-concept. As known, silicon is not the ideal hinge material due to its stiffness and brittleness which limits the amount of torsion the hinge can experience before mechanical failure. Polymers are being investigated to replace silicon for the hinge material due to their greater flexibility as was shown in [1].

2. Antenna Design

The Ansoft High Frequency Structure Simulator (HFSS) package is used to design the antenna and platform shown in Fig. 1. The antenna is required to have a broad bandwidth to allow frequency hopping for detection and imaging applications and capable of dual linear polarization for full manipulation of the polarimetric concept [6]. The antenna and platform must also be planar to be compatible with bulk micromachining techniques available at the High Density Electronics Center (HiDEC) at the University of Arkansas.

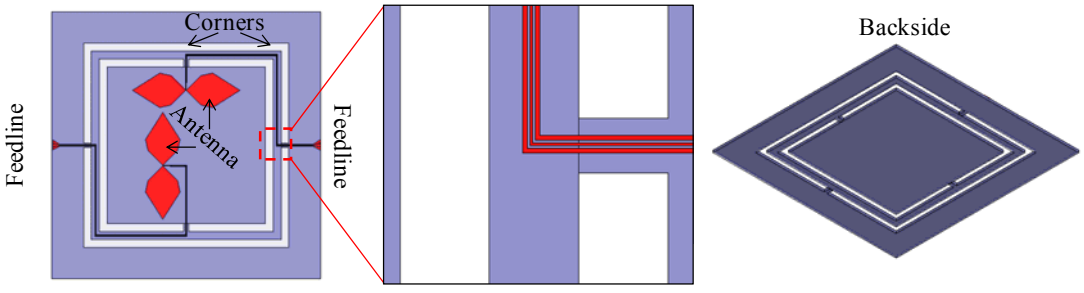

Fig. 1. MEMS Antenna design shown from the a) top view b) zoomed on the outer hinge and c) platform without antenna.

An antenna is designed to meet the requirements by modifying the Fourpoint antenna [7-8]. The substrate material is silicon with relative permittivity ε_r = 11.9 and 3μm thick silicon dioxide layer of ε_r = 4.5 to minimize substrate losses. The platform is made to be 9mm × 9mm to allow for a reasonable amount of rotation and to operate below 26.5 GHz since it is the limit of the available vector network analyzer.

The fabricated antenna shown in Figure 1 achieves a bandwidth of 41% and operates between ~10-16 GHz as will be shown in Section 4. The CPW feedline was designed with a signal line width 15μm a spacing of 9μm and a ground width of 25μm. Hinges of width 100μm, were designed such that the CPW feeding each antenna were routed across the nearest hinges to that antenna. The transition from the CPW to the SMA connector required flared contact pads for adhesion of the SMA connector. The CPW feed line is designed for a 50 Ω characteristic impedance. This design has led to having four corners associated with one antenna and three corners associated with the other antenna as shown in Fig. 1.

3. Device Fabrication

The MEMS platform was created using traditional bulk micromachining processes that are common in semiconductor manufacturing. The device was fabricated using a highly doped silicon <100> p-type wafer with a double sided polish (DSP), which is necessary since processing is required on both sides of the wafer. The metallic traces used to define the antenna shape included three layers of deposited metals; 500nm of titanium on the bottom, 2μm of copper in the middle, and 500nm of titanium on the top. The bottom titanium layer serves as adhesion for the copper layer while the top titanium layer eliminates the typical rapid oxidation of the copper.

The MEMS antenna significantly capitalized on the precision thickness controls that micromachining offers. Very thin layers of titanium were necessary for adhesion and to stop oxidation while a thicker copper layer served as the radiating element. It is important to minimize the thickness of the titanium layers since their electrical properties are not as good as copper and the overall thickness of the three layers affect the radiating characteristics of the device.

Fabrication consists of four major process steps outlined in Fig 2. Initially, through-holes must be etched into the bare silicon wafer depicted in Fig. 2a to serve as alignment marks. The through-holes are etched using Deep Reactive Ion Etching (DRIE) to create holes with a high depth to diameter ratio. Multiple holes are created with diameters ranging from 50-100 μm to ensure that clearly defined holes are available for alignment on both sides of the wafer. These vias allow for the alignment of features on both sides of the substrate in the absence of a double-sided aligner. This process is similar to what was done on early work with accelerometers.

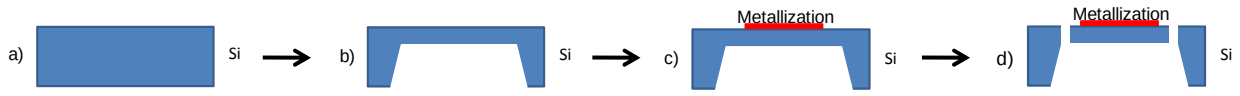

Fig. 2. Simplified fabrication process flow showing a) bare silicon wafer b) backside cavity etch c) metallization patterning for antenna and d) platform release

The underside of the wafer is then etched to create a cavity below the antenna platform as shown in Fig. 2b. The slope on the underside of the platform is not of critical importance so wet etching was utilized due to the ability to use batch processing. The roughness on the underside of

the platform and hinges, however, is very important as it creates stress points that can cause device failure. To minimize surface roughness a variety of wet etching techniques were explored with the best results achieved with Tetramethylammonium Hydroxide (TMAH).

Once the cavity on the underside is created, the metallization defining the antenna and coplanar waveguide feeding is deposited as shown in Fig 2c. The deposition was accomplished using the Sputtering process and patterned using standard photolithographic techniques. The metallization is then protected by a layer of photoresist to ensure that the tightly controlled metallization is not changed during the final etching step.

When the metallization is protected, the platform is released using DRIE as shown in Fig. 2d. This step etches out the trenches that connect to the cavity defined by the backside etch. DRIE is used to allow for precise control over the shape of the hinges which is vital to allow accurate control of the final device and to reduce any unintentional modifications to the metallization.

The individual devices are diced using a diamond scribing blade and the SMA connectors are attached using H20E two-part silver epoxy. The SMA connector was placed so that the center conductor lined up with the central pad and additional epoxy was added as needed to connect the outer pads to the ground on the SMA connector. The whole device was then placed in an annealing over at 150°C for one hour to cure the epoxy. At this stage the device is ready for testing and can be seen in Figure 3.

Fig. 3. Photo of two final devices ready for testing after the SMA connectors are attached using H20E epoxy.

4. Antenna Measurements

Measurements were made using a HP 8510C Vector Network Analyzer (VNA) in a 1m × 1m × 1m custom built anechoic chamber. This 2-port VNA model allows for measurement of the complex (magnitude and phase) transmission and reflection coefficients in a frequency sweep from 45MHz to 26.5GHz with up to 801 points per sweep. An 85052C 3.5mm precision calibration kit is used to move the measurement plane to the end of the cables. The data is transferred from the VNA to a desktop PC using a customized LabVIEW program. The anechoic chamber was built by students in the group, including the author, using standard plywood lined with pyramidal absorbing material purchased from ETS-Lindgren. The EMC Anechoic Absorber (model EMC-24CL) is designed to be useable in applications ranging from 60 MHz to 40 GHz with a guaranteed reflection of less than -50dB in the frequency range of 2-18 GHz. In addition to minimizing reflection from unintended objects, the chamber serves to reduce the amount of superfluous background radiation emitted from other equipment in the lab. The

anechoic chamber was previously used to collect scattered electromagnetic data for the reconstruction of metallic pipes suspended in air [9].

The measured and simulated S_{11} of the antenna elements is shown in Fig. 4 showing good agreement between the HFSS simulations and the measurements. The matching remains good while the antenna is rotated to 7º using a physical force. As the rotation increases the matching degrades slightly although it remains below -10dB for the small rotation that was achieved with the preliminary design. Increasing the amount of rotation could decrease the matching.

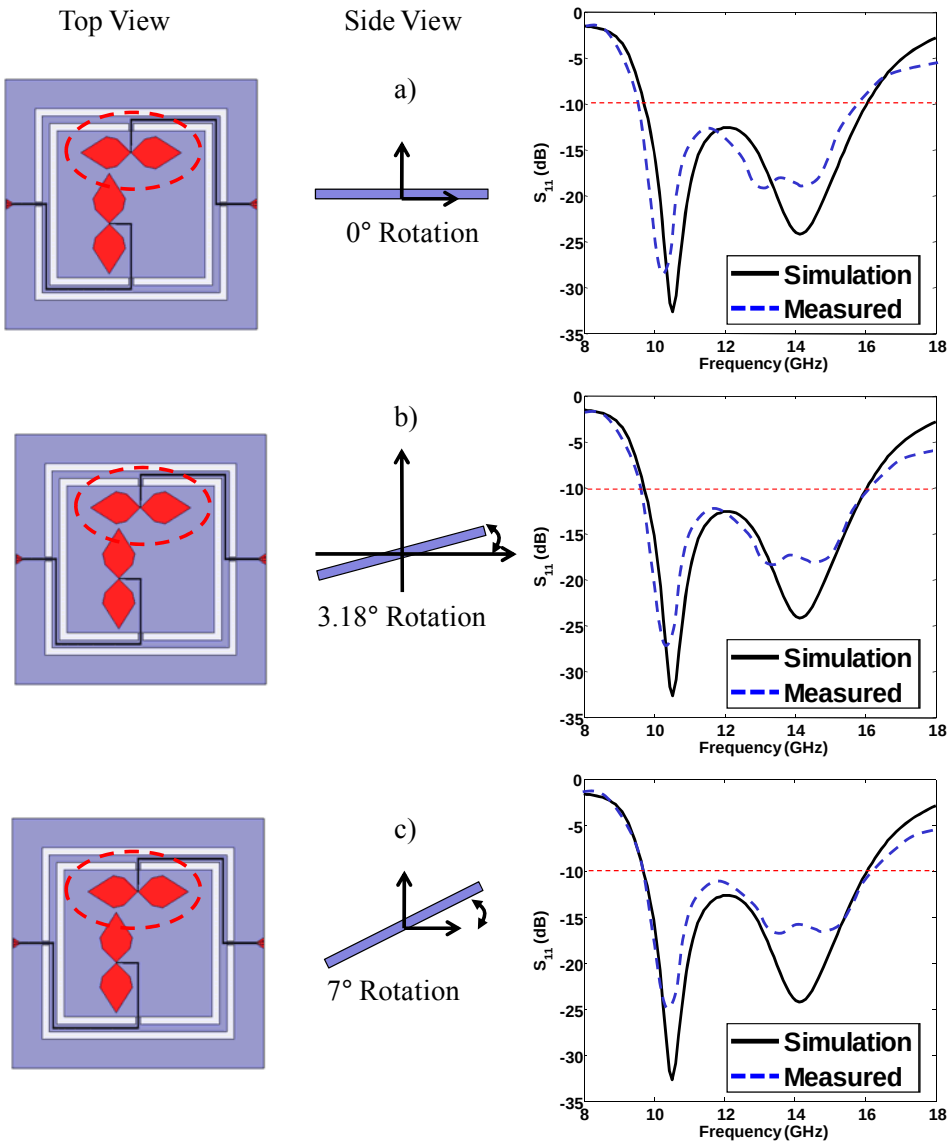

Fig. 4. Top and side views of the HFSS model and the measured and simulated S_{11} of the antenna with a) 0º rotation b) 3.18º rotation and c) 7º rotation.

5. Conclusions

A broadband silicon MEMS antenna was fabricated that operates between ~10 GHz and 16 GHz with a bandwidth of 41%. The measured and simulated S-parameters were in good agreement and the fabricated antenna was shown to provide maximum rotation around each axis of 9.14°. The integration of a broadband antenna with a MEMS platform allows additional degrees of freedom to control steering the beam of the array. Further optimization of the hinge geometry and the integration of polymer as the hinge material can increase the amount of rotation possible.

6. Acknowledgements

This work funded in part by the National Science Foundation Graduate Research Fellowship, National Science Foundation GK-12 Program and National Science Foundation Award Number ECS – 0524042.

References

[1] C. Baek, S. Song, J. Park, S. Lee, J. Kim, W. Choi, C. Cheon, Y. Kim and Y. Kwon, "A V-Band Micromachined 2-D Beam-Steering Antenna Driven by Magnetic Force with Polymer-Based Hinges," *IEEE Trans. Microwave Theory and Tech.*, Vol. 51, No. 1, pp. 325-331, Jan. 2003.

[2] X. Yang, B. Wang, Y. Zhang, "A Reconfigurable Hilbert Curve Patch Antenna," *IEEE Antennas and Propagation Society International Symposium,* Vol. 2B, pp. 613 – 616, 3-8 July 2005.

[3] E. Erdil, K. Topalli, M. Unlu, O.A. Civi, T. Akin, "Frequency Tunable Microstrip Patch Antenna Using RF MEMS Technology," *IEEE Trans. Antennas and Propagation,* Vol. 55, No. 4, pp. 1193 – 1196, April 2007.

[4] G.E. Ponchak, R.N. Simons, M. Scardelletti, "Microelectromechanical switches for phased array antennas," *IEEE Antennas and Propagation Society International Symposium,* Vol. 4, pp. 2230 – 2233, 16-21 July 2000.

[5] S.Y. Suh, "A Comprehensive Investigation of New Planar Wideband Antennas," PhD Dissertation, Virginia Polytechnic Institute, Blacksburg, VA, USA, 2002.

[6] M. El-Shenawee, "Polarimetric Scattering From Two-Layered Two-Dimensional Random Rough Surfaces With and Without Buried Objects," *IEEE Trans. Geoscience and Remote Sensing*, Vol. 42, No. 1, pp. 67-76, Jan. 2004.

[7] D. Woten, M. El-Shenawee and S. Tung, "Planar Broadband Dual-Linearly Polarized MEMS Steerable Antenna," *Proc. of the IEEE 2009 AP-S International Symposium*, Charleston, South Carolina, June 1-5, 2009.

[8] D. A. Woten and M. El-Shenawee, "Broadband Dual Linear Polarized Antenna for Statistical Detection of Breast Cancer," *IEEE Trans. Antennas and Propagation*, Vol. 56, No. 11, pp. 3576-3580, Nov. 2008.

[9] D. Woten, R. M. Hajihashemi, A. Hassan and M. El-Shenawee, "Experimental Microwave Validation of Level-Set Reconstruction Algorithm*," IEEE Trans Antennas and Propagation*, Accepted for Publication in Jan 2010.